THE JOURNAL OF BIOLOGICAL CHEMISTRY
Vol. 276, No. 31, Issue of August 3, pp. 29019–29027, 2001

Printed in U.S.A.

Ultrastructure and Function of Dimeric, Soluble Intercellular Adhesion Molecule-1 (ICAM-1)*

Received for publication, April 17, 2001, and in revised form, June 4, 2001
Published, JBC Papers in Press, June 4, 2001, DOI 10.1074/jbc.M103394200

Chang-Duk Jun†¶, Christopher V. Carman†¶, Sambra D. Redick§, Motomu Shimaoka‡, Harold P. Erickson§, and Timothy A. Springer†‖

From the Center for Blood Research and the Departments of †Pathology and ‡Anesthesia, Harvard Medical School, Boston, Massachusetts 02115 and the §Department of Cell Biology, Duke University Medical Center, Durham, North Carolina 27710

Previous studies have demonstrated dimerization of intercellular adhesion molecule-1 (ICAM-1) on the cell surface and suggested a role for immunoglobulin superfamily domain 5 and/or the transmembrane domain in mediating such dimerization. Crystallization studies suggest that domain 1 may also mediate dimerization. ICAM-1 binds through domain 1 to the I domain of the integrin $\alpha_L\beta_2$ (lymphocyte function-associated antigen 1). Soluble C-terminally dimerized ICAM-1 was made by replacing the transmembrane and cytoplasmic domains with an α-helical coiled coil. Electron microscopy revealed C-terminal dimers that were straight, slightly bent, and sometimes U-shaped. A small number of apparently closed ring-like dimers and W-shaped tetramers were found. To capture ICAM-1 dimerized at the crystallographically defined dimer interface in domain 1, cysteines were introduced into this interface. Several of these mutations resulted in the formation of soluble disulfide-bonded ICAM-1 dimers (domain 1 dimers). Combining a domain 1 cysteine mutation with the C-terminal dimers (domain 1/C-terminal dimers) resulted in significant amounts of both closed ring-like dimers and W-shaped tetramers. Surface plasmon resonance studies showed that all of the dimeric forms of ICAM-1 (domain 1, C-terminal, and domain 1/C-terminal dimers) bound similarly to the integrin $\alpha_L\beta_2$ I domain, with affinities ~1.5–3-fold greater than that of monomeric ICAM-1. These studies demonstrate that ICAM-1 can form at least three different topologies and that dimerization at domain 1 does not interfere with binding in domain 1 to $\alpha_L\beta_2$.

Intercellular adhesion molecule-1 (ICAM-1,[1] CD54) is the most important of a group of related immunoglobulin superfamily (IgSF) molecules that serve as ligands for the integrin $\alpha_L\beta_2$ (1). ICAM-1 is expressed basally on the surface of cells important in immune responses. Its expression is enhanced further on these cells and induced on other cell types, including endothelial, epithelial, and fibroblastic cells, by inflammatory mediators. Increased ICAM-1 expression augments immune responses and leukocyte accumulation in inflamed tissues. ICAM-1 contains a binding site for $\alpha_L\beta_2$ in domain 1 and a binding site for the related leukocyte integrin $\alpha_M\beta_2$ in domain 3. ICAM-1 is also subverted by the major group of rhinoviruses as a receptor for entry into nasal epithelial cells and by *Plasmodium falciparum* for sequestration of infected erythrocytes in the peripheral vasculature.

ICAM-1 consists of five extracellular IgSF domains (domains 1–5), a hydrophobic transmembrane domain, and a short cytoplasmic domain (1) (see Fig. 1). Electron micrographs of truncated, soluble ICAM-1 (sICAM-1) show that its five IgSF domains assume a rod-like shape 18.7 nm in length, with a characteristic bend ~11 nm from the N terminus between domain 3 (D3) and domain 4 (D4) (2, 3). Crystal structures have been determined for domains 1 and 2 of ICAM-1 (4, 5). The binding site for $\alpha_L\beta_2$ has been identified in ICAM-1 by mutagenesis and is located near the middle of domain 1 on the edge of the β-sandwich (2). The binding surface is slightly convex, and the most important residue is Glu-34, located in an edge β-strand. $\alpha_L\beta_2$ must be activated by conformational change or clustering in the membrane to be adhesive for ICAM-1 (6). An inserted (I) domain in the integrin α_L subunit appears to bind directly to ICAM-1. The I domain bears a Mg^{2+} ion that is hypothesized to ligate Glu-34 of ICAM-1. Conformational movements in the I domain have been demonstrated to alter dramatically its adhesiveness and affinity for ICAM-1 (7–9).

ICAM-1 appears to exist as a dimer and higher multimers in its native state on the cell surface, as shown by cross-linking studies (10, 11); however, the architecture of these multimers is unknown. Soluble ICAM-1 can be dimerized in fusion proteins, and this increases its avidity for $\alpha_L\beta_2$ and rhinovirus (11–13). However, the function of dimerization in the context of native, cell surface-expressed ICAM-1 remains to be determined.

Multiple modes of dimerization have been suggested for ICAM-1. Previous cross-linking studies have suggested that domain 5 and/or the transmembrane domain can mediate dimerization (10, 11). In addition, a crystal structure of domains 1 and 2 of ICAM-1 revealed a putative dimerization interface on the face containing β-strands B, E, and D (BED sheet) of domain 1. The $\alpha_L\beta_2$ binding interface is on the opposite side of domain 1 from the dimerization interface, such that the two Glu-34 residues are far from one another and pointing away from the interface. It was hypothesized that two $\alpha_L\beta_2$ molecules could bind simultaneously to the dimer (4). The domain 1 dimerization interface contains at its center hydrophobic residues including leucines 18, 42, 43, and 44 (4). Its

* The costs of publication of this article were defrayed in part by the payment of page charges. This article must therefore be hereby marked "*advertisement*" in accordance with 18 U.S.C. Section 1734 solely to indicate this fact.

¶ These authors contributed equally.
‖ To whom correspondence should be addressed: Dept. of Pathology, Harvard Medical School, 200 Longwood Ave., Boston, MA 02115. Tel.: 617-278-3200; Fax: 617-278-3232; E-mail: springer@sprsgi.med.harvard.edu.

[1] The abbreviations used are: ICAM-1, intercellular adhesion molecule-1; IgSF, immunoglobulin superfamily; sICAM-1, soluble ICAM-1; I domain, inserted domain; FBS, fetal bovine serum; CHO, Chinese hamster ovary; mAb, monoclonal antibody; PCR, polymerase chain reaction; bp, base pair; PAGE, polyacrylamide gel electrophoresis; DTT, dithiothreitol, LFA, lymphocyte function-associated antigen.

hydrophobicity suggests that this interface might be biologically relevant (14). However, the size of this interface is insufficient to drive strong dimerization, leaving its physiologic relevance inconclusive. Furthermore, in another crystal study with domains 1 and 2 of ICAM-1 in which three *N*-linked glycosylation sites were mutated, this dimer interface was not seen (5). Instead, a hydrophilic dimer interface, such as is commonly found in crystal lattice contacts, was seen.

Thus far, it has not been clear whether the C-terminal and domain 1 dimer interfaces are structurally compatible with one another. Could dimerization occur at both interfaces simultaneously? Furthermore, what would be the nature of such dimers? One way to reconcile dimerization in domain 1 with dimerization near domain 5 or the transmembrane domain would be if dimerization at these regions occurred in *cis*, with formation of a closed, ring-like dimer (4). On the other hand, dimerization might occur in *trans*, linking different pairs of molecules at each interface. Furthermore, it has not yet been established whether domain 1 can, in fact, support dimerization. Moreover, it is not clear whether and how the maintenance of structural constraints by dimerization via domain 1 or the transmembrane domain would affect binding to $\alpha_L\beta_2$. In this study, we have investigated these issues.

MATERIALS AND METHODS

Cell Lines and Antibodies—293T cells (a human renal epithelial transformed cell line) were grown in Dulbecco's modified Eagle's medium (Life Technologies, Inc.) supplemented with 10% FBS, nonessential amino acids (Life Technologies, Inc.), and 50 μg/ml of gentamicin. CHO-K1 cells were maintained in Ham's F-12K medium, 10% FBS, and 50 μg/ml penicillin/streptomycin. CHO.Lec 3.2.8.1 cells (a glycosylation-defective variant of CHO-K1 cells) and SKW3 cells were maintained as described previously (13, 15). mAbs R6.5 (16), CA-7 (17), CL203 (18), and CBRIC1/11 (19) have been described previously. Within ICAM-1, mAb R6.5 maps to domain 2 (2), mAb CBRIC1/11 maps to domain 3 (19), mAb CL203 maps to domain 4 (2), and mAb CA-7 maps to domain 5 (17).

cDNA Constructions—The human wild-type ICAM-1 cDNA (20) was subcloned into the *Hin*dIII and *Not*I restriction sites of the pAprM8 vector (21) to generate ICAM-1/pAprM8. For the C-terminal dimer, cDNA encoding domains 1–5 of ICAM-1 was fused to the α-helical coiled coil domain of the yeast transcription factor GCN4 containing a disulfide-promoting cysteine substitution (22, 23) by overlap extension PCR. In the first PCR, using ICAM-1/pAprM8 as template, a 260-bp fragment was generated which included an internal ICAM-1 *Bgl*II site and codons for the last amino acids of the ICAM-1 ectodomain (SPRYE) fused with the first amino acids (RMKQCLEDKVEEL*LSKNYHL*) of the GCN4-p1 peptide. In the second PCR, also using ICAM-1/pAprM8 as a template, an ~200-bp fragment was generated, which included a sequence encoding the last C-terminal amino acids (*LSKNYHL*ENEVARLKKLVG) of the GCN4-p1 peptide, a stop codon, and a 170-bp nontranslated ICAM-1 sequence followed by a vector 3′-*Not*I site. In the final PCR, the 260- and ~200-bp fragments were used together as overlapping templates (region of overlap indicated by the italicized GCN4-p1 residues shown above) to prepare an ~460-bp product. After digestion with *Bgl*II and *Not*I, this product was used to replace the corresponding wild-type sequence of ICAM-1 in the ICAM-1/pAprM8 vector, thus giving rise to the mutant plasmid sICAM-1_GCN4/pAprM8.

For domain 1 dimers, Protein Data Bank files were made from accession 1ic1 containing the crystallographic symmetry-related dimers of the A or B molecules (4). Residues near the dimer interface which might form disulfide bonds if mutated to cysteine were identified with the program SSBOND (24) or by visual inspection with LOOK (25). A three-round PCR method for single site-specific mutagenesis was performed to introduce cysteine mutations. Briefly, 5′- and 3′-primers were designed to include unique restriction sites that were used in two separate PCRs with a pair of mutagenic inner complementary primers. The resulting overlapping products were used as the template for the third PCR, the product of which was digested and ligated into the corresponding predigested plasmids.

The cDNA encoding soluble monomeric ICAM-1 (sICAM-1/pAprM8) was described previously (26). To generate stable cell lines, all mutant cDNAs were subcloned further into the *Bam*HI and *Not*I sites of pEF1/V5_puro vector (27), a modified vector from pEF1/V5_neo. All constructs were verified by DNA sequencing. A schematic representation of the ICAM-1 constructs used in this study is depicted in Fig. 1.

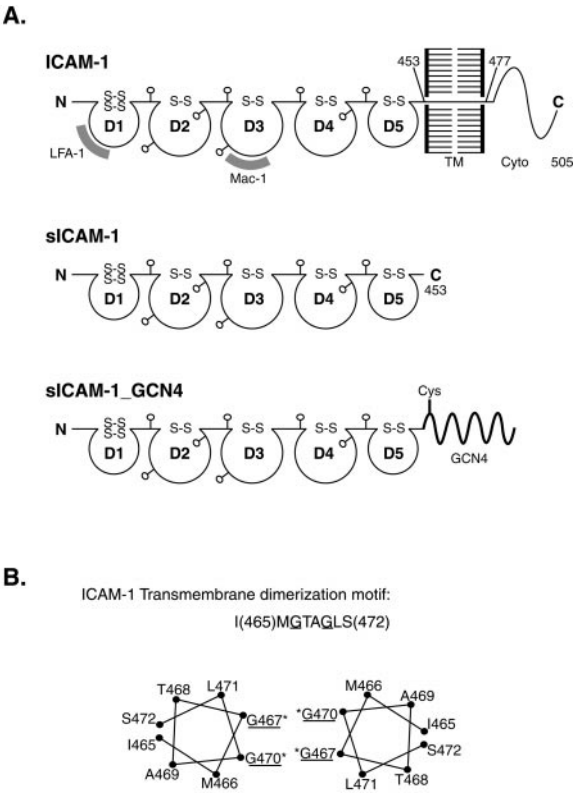

FIG. 1. **Schematic representation of C-terminally mutated ICAM-1 constructs and a putative transmembrane domain dimerization motif.** *Panel A*, wild-type ICAM-1, ICAM-1 truncated prior to the transmembrane domain (sICAM-1), and ICAM-1 with a GCN4 α-helical coiled coil dimerization motif and a cysteine to link the coiled coils covalently (sICAM-1_GCN4). IgSF domains 1–5 (*D1–D5*) are schematized as loops closed by intradomain disulfide (*S-S*) bonds. *Lollipops* represent *N*-linked glycosylation sites. *TM*, transmembrane domain; *Cyto*, cytoplasmic domain. *Panel B*, helical wheel representation of the last portion of the putative α-helical ICAM-1 transmembrane domain.

cDNA Transfections—Proteins were expressed transiently in 293T or CHO.Lec 3.2.8.1 cells using FuGENE™ 6 transfection reagent according to the manufacturer's instructions (Roche Molecular Biochemicals, Indianapolis, IN) (13, 28). Stable cell lines that express soluble monomeric or dimeric ICAM-1 were generated by FuGENE™ 6-mediated transfection of 2 μg of various ICAM-1/pEF1/V5_puro constructs into CHO.Lec 3.2.8.1 cells, followed by selection with 10 μg/ml puromycin beginning at 48 h post-transfection. All stable cell lines were maintained in complete medium supplemented with the same concentrations of antibiotic.

Radiolabeling and Immunoprecipitation—Metabolic labeling and immunoprecipitation were described previously (29). Briefly 5×10^6 cells in 4 ml of labeling medium (cysteine/methionine-free RPMI containing 15% dialyzed FBS) were labeled with 0.5 mCi of [^{35}S]cysteine and methionine (ICN Biochemicals) overnight at 37 °C. Labeled cell culture supernatants (500 μl) were then incubated with R6.5 (an ICAM-1 domain 3-specific mAb) coupled at 3 mg/ml to Sepharose CL-4B beads (50 μl of a 1:1 slurry) for 3 h at 4 °C. The immunoprecipitates were analyzed by SDS-PAGE (10% gel) (with or without 10 mM DTT) and fluorography.

Protein Purification—The purification of monomeric and dimeric ICAM-1 was carried out at 4 °C. Culture supernatant (2 liters) containing ICAM-1 was passed through a CBRIC1/11 mAb Sepharose CL-4B affinity column (30 ml at 2 mg/ml) followed by extensive washing with 10 mM Tris-HCl, pH 8.0, containing 0.15 M NaCl. Bound proteins were eluted with 50 mM triethylamine, pH 11.5, containing 0.15 M NaCl, and fractions were collected in test tubes containing 1/10 volume of 1 M Tris-HCl, pH 6.5, to neutralize the pH. For Mono Q column chromatography, the protein samples and column were equilibrated with 20 mM Tris, pH 8.0, and eluted using a linear gradient of 0–1 M NaCl. For size exclusion chromatography, the samples were passed over a Superdex-200 column in PBS.

Antibody Binding Assay—mAbs R6.5 and CA-7 were adsorbed separately to the wells of a flat bottom 96-well polystyrene plate (Flow Laboratories, McLean, VA) by incubation overnight at 4 °C. Nonspecific binding sites were blocked with 1% heat-treated bovine serum albumin for 1 h at 37 °C. sICAM-1 or sICAM-1_GCN4 (500 ng/ml in PBS) was then added to the wells and incubated for 30 min at 37 °C followed by washing three times with PBS. Binding of sICAM-1 and sICAM-1_GCN4 was detected by incubation with biotin-conjugated CBRIC1/11 mAb followed by washing with PBS and addition of streptavdin-conjugated horseradish peroxidase and 2,2′-azinobis(3-ethylbenzthiazoline-6-sulfonic acid)-diammonium salt as substrate. Absorbance at 414 nm was then measured.

Gradient Sedimentation and Electron Microscopy—Proteins were subjected to glycerol gradient sedimentation, and sedimentation coefficients were obtained as described previously (30). Rotary-shadowed specimens were prepared directly from gradient fractions and subjected to electron microscopy as described (30).

Determination of Binding Constants for Soluble Monomeric or Dimeric ICAM-1 by Surface Plasmon Resonance—The binding of a designed mutant (K287C/K294C) of the $\alpha L\beta 2$ I domain, which is locked in the high affinity open conformation (open $\alpha L\beta 2$ I domain) to ICAM-1 was monitored with a BIAcore 1000 instrument (BIAcore, Piscataway, NJ), as described previously (8). Briefly, open $\alpha L\beta 2$ I domain or bovine serum albumin (control) proteins were covalently immobilized onto sensor chips, and ICAM-1 dimers or monomers were flowed over the sensor chips. k_{on} and k_{off} values were obtained by curve fitting of the association and dissociation phases of sensograms, respectively, using either a 1:1 binding model for monomeric ICAM-1 or a bivalent analyte binding model for dimeric ICAM-1 using BIAevaluation software (BIAcore). K_D was then calculated from k_{on} and k_{off} ($K_D = k_{off}/k_{on}$).

Homotypic Aggregation Assay—Because the LFA-1/ICAM-3 interaction is slightly less efficient than that of LFA-1/ICAM-1 (15), ICAM-1 is expected to compete efficiently with ICAM-3 for LFA-1 binding. SKW3 cells undergo LFA-1- and ICAM-3-dependent homotypic aggregation (15). The ability of soluble forms of ICAM-1 to bind cell surface LFA-1 can, therefore, be monitored sensitively as inhibition of SKW3 homotypic aggregation. Thus, SKW3 cells were dissociated by washing in Ca^{2+}/Mg^{2+}-free PBS and then resuspended in L15 medium containing 2.5% FBS (L15/FBS) at 2×10^6 cells/ml. The cells were then combined with 10 μg/ml of the $\alpha_L\beta_2$ activating mAb CBR-LFA1/2, and 50 μl/well was added to 96-well microtiter plates containing 50 μl of L15/FBS with 0–4 μM monomeric ICAM-1 or domain 1 dimeric, C-terminal dimeric, or domain 1/C-terminal dimeric ICAM-1 and incubated 30 min at 37 °C. Samples were then visualized via light microscopy, and aggregation was scored from 0 to 5 as described previously (31).

RESULTS

ICAM-1 Dimerized through a C-terminal GCN4 Coiled Coil—The transmembrane domain of ICAM-1 has glycine residues that cluster on one side of the predicted transmembrane α-helix and form a hydrophilic "bald" patch in the inner leaflet of the bilayer which is postulated to mediate dimerization (Fig. 1*B*) (10). To mimic dimerization through lateral association of α-helical transmembrane domains, we fused a water-soluble α-helical coiled coil to the C terminus of the extracellular domain (sICAM-1_GCN4; Fig. 1). The four heptad repeats of the yeast GCN4 protein were used, which form an α-helical coiled coil homodimer. A cysteine was used in the fourth position of the first heptad repeat to stabilize the homodimer further by formation of a disulfide bond (23). sICAM-1_GCN4 was expressed and labeled metabolically in 293T cells and subjected to immunoprecipitation, SDS-PAGE, and fluorography (Fig. 2*A*). Disulfide-linked sICAM-1_GCN4 dimers were made efficiently, as confirmed by the presence of an ~180-kDa dimeric band and an ~90-kDa monomeric band in the absence and presence of reduction with DTT, respectively (Fig. 2*A*). The yield of sICAM-1_GCN4 dimer was similar to that of sICAM-1 monomer, which migrated at ~90 kDa under both reducing and nonreducing conditions (Fig. 2*A*).

The mAb CA-7 is specific for domain 5 of ICAM-1 (17). It reacts well with ICAM-1 with an artificial glycosylphosphatidylinositol anchor but poorly with native cell surface ICAM-1, and it recognizes domain 5 of ICAM-1 in monomeric but not dimeric ICAM-1 (11). To examine reactivity with CA-7 mAb, sICAM-1_GCN4 and sICAM-1 were expressed in CHO.Lec 3.2.8.1 cells, purified, and compared for binding to CA-7 mAb and R6.5 mAb (a dimerization-independent mAb to domain 2) in a capture enzyme-linked immunosorbent assay (Fig. 2*B*). Interestingly, sICAM-1 was recognized equally well by CA-7 and R6.5 mAbs, whereas sICAM-1_GCN4 was recognized poorly by CA-7 compared with R6.5. When similar peptides are fused to the C terminus which do not result in dimerization, the CA-7 epitope is not shielded.[2] Thus the CA-7 epitope is shielded both in sICAM-1_GCN4 dimers and in native ICAM-1 dimers on the cell surface, suggesting that the disposition of domain 5 is similar in both and that sICAM-1_GCN4 dimers may mimic cell surface dimers.

Purified preparations of sICAM-1 and sICAM-1_GCN4 C-terminal dimers were characterized further by glycerol gradient sedimentation, rotary shadowing, and electron microscopy.

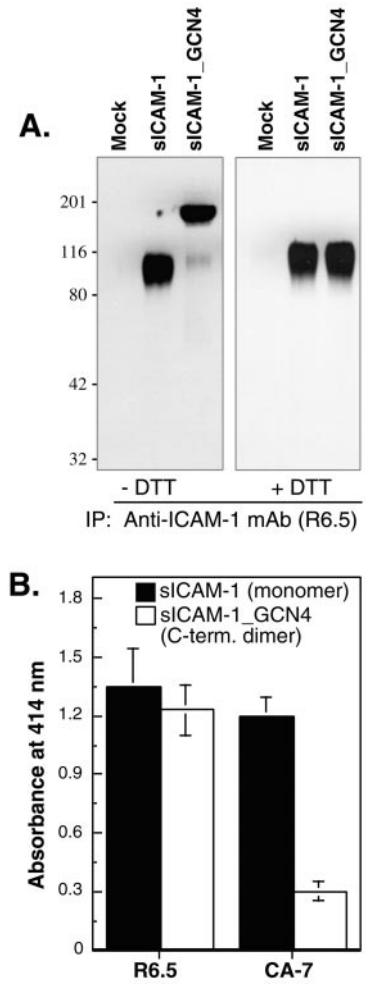

FIG. 2. **Generation and characterization of C-terminally dimerized ICAM-1 (sICAM-1_GCN4).** *Panel A*, 293T cells transfected with the indicated constructs were labeled with [^{35}S]methionine and cysteine, and secreted material was immunoprecipitated with R6.5 mAb. Samples were subjected to SDS-PAGE (10% gel) under nonreducing (−*DTT*) or reducing conditions (+*DTT*) and fluorography. *Panel B*, sICAM-1 (monomer) and sICAM-1_GCN4 (C-terminal dimer) were tested at 500 ng/ml for binding to immobilized R6.5 (a dimerization-independent ICAM-1 mAb) or CA-7 (a monomer-specific mAb). Binding was determined by the addition of biotin-conjugated CBRIC1/11 mAb followed by enzyme-linked immunosorbent assay and measurement of absorbance at 414 nm. Values represent the mean ± S.E. for at least three separate experiments.

[2] C. D. Jun, C. V. Carman, and T. A. Springer, unpublished data.

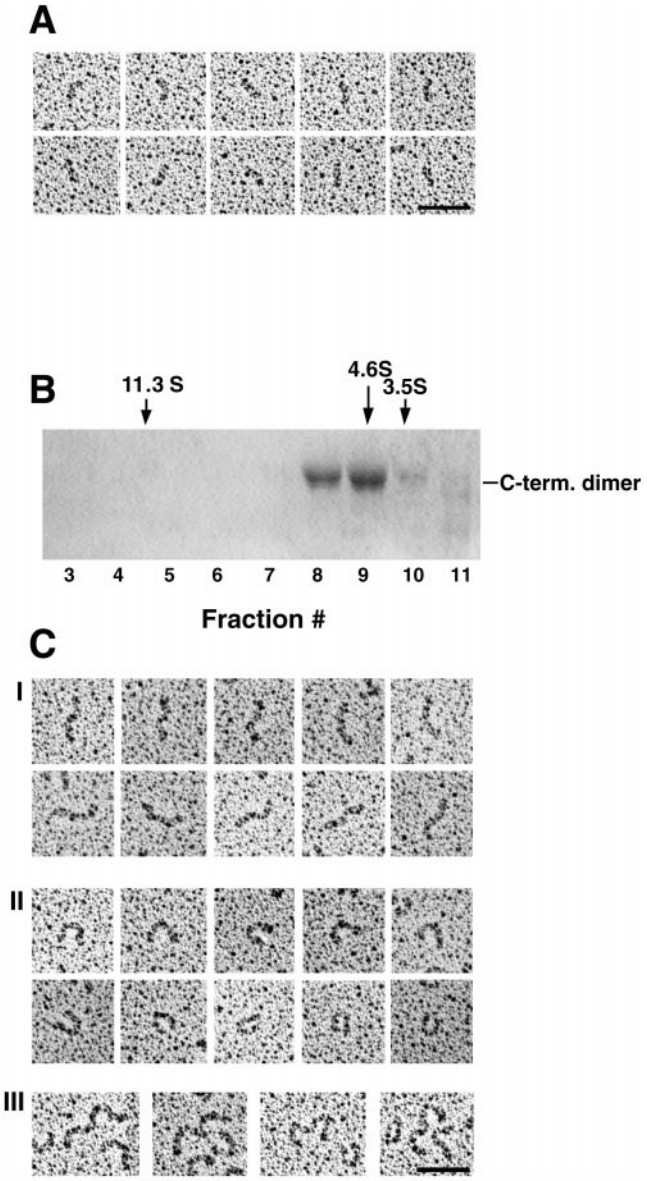

FIG. 3. **Purification and visualization of C-terminal dimers.** *Panel A*, representative electron micrographs of purified and rotary-shadowed sICAM-1. *Bar* = 50 nm. *Panel B*, purified sICAM-1_GCN4 C-terminal dimer was sedimented through a glycerol gradient, and fractions were subjected to SDS-PAGE (10% gel) and staining. The positions of standards sedimented in a parallel gradient are shown above the gel; fraction numbers are shown below the gel. *Panel C*, gradient-purified C-terminal dimers were subjected to rotary shadowing and electron microscopy. Representative extended dimers (*rows I*), U-shaped and ring-like dimers (*rows II*), and W-shaped tetramers (*rows III*) are depicted.

In good agreement with previous studies (2, 3) sICAM-1 appeared as a slightly bent rods ~18 nm in length (Fig. 3*A*). The sICAM-1_GCN4 preparation sedimented on a glycerol gradient with a sedimentation coefficient of 5.5 S (Fig. 3*B*). Rotary-shadowed electron micrographs confirmed that sICAM-1_GCN4 was dimeric. Its contour length was 33–43 nm, about twice that of sICAM-1. Most of the sICAM-1_GCN4 dimers were extended (Fig. 3*C*, *rows I*). About 10–20% of the molecules showed a pronounced bend into a symmetrical U shape, and rarely the two ends of the U were in contact, forming a circle (Fig. 3*C*, *rows II*).

The circles and Us suggest that noncovalent domain 1/domain 1 interactions might occur by bending a GCN4 dimer to bring its ends into contact. If this interaction were stable it should produce circles, but the U-shaped molecules suggest that most circles are disrupted and the ends separated somewhat. We believe that this disruption happens as the molecules are deposited on the mica. There are at least two precedents for noncovalent protein-protein bonds being disrupted in this fashion. Rotary-shadowed dimeric factor XIIIa appeared as two variably separated subunits, only rarely in contact, suggesting that the subunits separated and moved apart after being deposited on the mica (32). A recent study of cell adhesion molecule L1 provided evidence that it was folded into a horseshoe conformation in solution, but after deposition on mica the horseshoe unfolded into an elongated conformation (33). The small number of W-shaped molecules suggests that domain 1 association can also occur between two GCN4 dimers (Fig. 3*C*, *row III*). These results encouraged us to design additional constructs to probe further the relationship of domain 1 and the segment following domain 5 to ICAM-1 dimerization and function.

TABLE I

Cβ–Cβ distances and exposure of symmetry-related residues in the domain 1 dimer interface seen in a crystal structure of domains 1 and 2 of ICAM-1

The putative dimerization interface in domain 1 was deduced from symmetry-related contacts seen between pairs of A molecules (A dimer) and B molecules (B dimer) in a crystal structure of ICAM-1 domains 1 and 2 (4). The distance separating the Cβ atoms of identical residues in the interface was measured. Surface accessibility of each of these residues in the absence of the interface, *i.e.* in monomer molecules, was measured as exposed surface area (Å^2) using the program DSSP (38).

Residue	Dimer Cβ–Cβ distance		Surface exposure	
	A dimer	B dimer	A monomer	B monomer
	Å		*Å^2*	
Leu-18	4.50	6.03	92	93
Leu-42	3.41	4.40	74	62
Leu-43	3.61	2.48	185	166
Leu-44	10.8	4.40	47	57

Cysteines Introduced into the Putative Dimerization Interface in Domain 1 Can Form Disulfide-linked sICAM-1 Dimers—sICAM-1 has been characterized previously as monomeric (11). The hydrophobic interface visualized in domain 1 in crystals might be sufficient to drive dimerization of native molecules on the cell surface (4) but is not sufficient to form stable sICAM-1 dimers in solution (11). We rationalized that transient dimers formed in solution might be "captured" if cysteines were introduced into the dimerization interface in positions where disulfide bond formation was compatible with an interface stabilized by noncovalent interactions. We measured the distances separating β-carbons (Cβ atoms) of pairs of residues in the interface between domain 1 visualized in the crystal structure of domains 1 and 2 of ICAM-1 (4) (Table I). There are two independent molecules in the asymmetric unit of these crystals, termed molecules A and B. Hydrophobic dimer interfaces lie between 2-fold symmetry-related A molecules and between 2-fold symmetry-related B molecules. There are small differences in the orientation at these two interfaces, and thus we measured distances at both (Table I). Symmetry-related Leu-42 and Leu-43 residues had Cβ atoms that were within the distance of 3.41–4.25 Å optimal for disulfide formation (24), and symmetry-related Leu-18 and Leu-44 residues had Cβ atoms that were somewhat farther apart. Each of these residues was accessible on the surface of ICAM-1 monomers (Table I). Thus when mutated to cysteine, all residues were predicted to be accessible for disulfide bond formation.

Each of these four residues was mutated to cysteine, and sICAM-1 variants containing the L18C, L42C, L43C, and L44C mutations were expressed in CHO.Lec 3.2.8.1 cells. CHO.Lec 3.2.8.1 cells are mutant for complex carbohydrate-processing

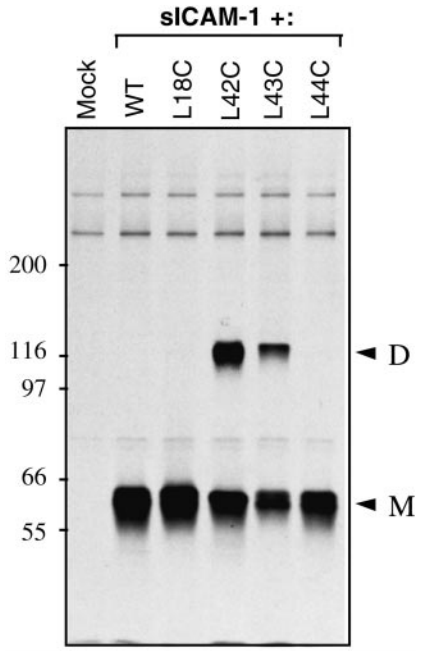

FIG. 4. **Generation of covalently dimerized sICAM-1 by formation of a disulfide bond in domain 1.** Secreted material from ^{35}S-labeled CHO.Lec 3.2.8.1 cells expressing the indicated wild-type (*WT*) or cysteine substitution mutants of sICAM-1 were assessed for disulfide formation by immunoprecipitation with R6.5 mAb, SDS-PAGE (10% gel) under nonreducing conditions, and fluorography. The molecular masses $\times 10^{-3}$ of standards are shown on the *left*, and the positions of dimer (*D*) and monomer (*M*) bands are shown on the *right*.

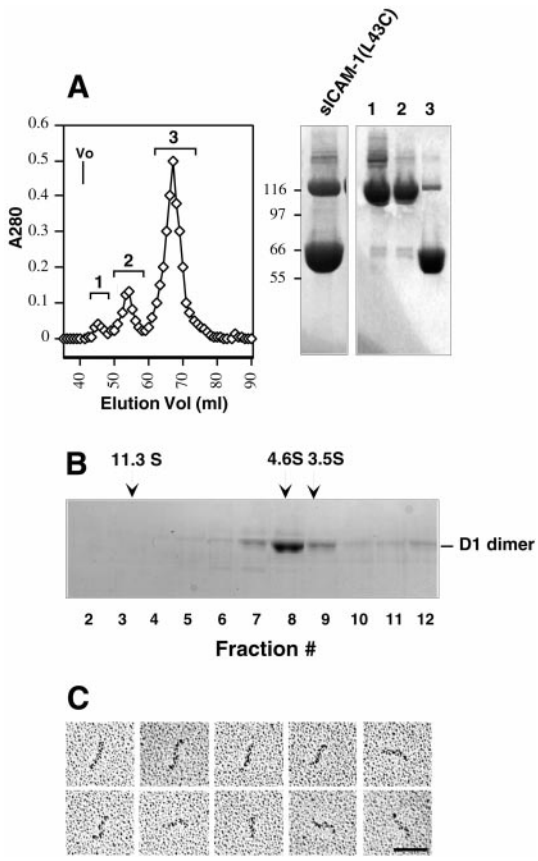

FIG. 5. **Characterization of domain 1 dimers.** *Panel A*, gel filtration and SDS-PAGE. sICAM-1(L43C) expressed in CHO.Lec 3.2.8.1 cells was purified by CBRIC1/11 mAb affinity column chromatography and subjected to gel filtration on a 2.5 × 50-cm Superdex-200 column (*left*). Pooled fractions representing peaks 1, 2, and 3 were concentrated and visualized by SDS-PAGE (10% gel) under nonreducing conditions (*right*). Fractions from peak 2 were used for further studies including sedimentation (*panel B*), electron microscopy (*panel C*), and BIAcore analysis (see Table II). *Panel B*, sedimentation. Purified sICAM-1(L43C) domain 1 dimers were sedimented through a glycerol gradient, and fractions were subjected to SDS-PAGE (10% gel) and Coomassie Blue staining. The positions of standards sedimented in a parallel gradient are indicated above the gel; gradient fraction numbers are indicated below the gel. *Panel C*, electron microscopy. Gradient-purified domain 1 dimers were subjected to rotary shadowing and electron microscopy. Representative images are depicted. *Bar* = 50 nm.

enzymes, and therefore the molecular masses of monomeric and dimeric ICAM-1 species were lower than when produced in 293T cells. The sICAM-1 L42C and L43C mutants formed disulfide-linked dimers, as shown by the presence of an ~115-kDa band in SDS-PAGE (Fig. 4). This band was completely converted to the monomeric size of ~58 kDa after reduction (data not shown). By contrast, L18C and L44C sICAM-1 molecules failed to form stable dimers (Fig. 4). This correlated with longer Cβ-Cβ distances but not with exposure on the monomer surface (Table I).

Dimeric L43C sICAM-1 was purified by immunoaffinity and gel filtration chromatography (Fig. 5*A*). Glycerol gradient sedimentation yielded a coefficient of 4.4 S (Fig. 5*B*). Electron micrographs of the dimers purified by sedimentation revealed rods 30–36 nm in length exhibiting extended or V-shaped topologies with a bend in the middle (Fig. 5*C*). Thus, stable disulfide-linked domain 1 dimers of ICAM-1 were formed, and these appeared to be guided by noncovalent contacts in the crystal-defined domain 1 interface because dimerization correlated with Cβ atom proximity in this interface.

Expression and Ultrastructure of sICAM-1 with Covalent Stabilization of Both C-terminal and Domain 1 Dimerization Motifs—We tested whether the U-like and ring-like dimers and the W-shaped tetramers observed with sICAM-1_GCN4 (Fig. 3*C*, *rows II* and *III*) could be stabilized. The disulfide-forming L43C cysteine substitution was introduced into the domain 1 dimerization interface together with C-terminal dimerization through the GCN4 coiled coil. The sICAM-1_GCN4(L43C) and sICAM-1_GCN4 constructs were expressed in CHO.Lec 3.2.8.1 cells, and radiolabeled material was subjected to immunoprecipitation and SDS-PAGE (Fig. 6*A*). sICAM-1_GCN4 yielded both monomeric and dimeric material as shown above, with molecular masses when produced by CHO.Lec 3.2.8.1 cells of 58 and 112 kDa, respectively (Fig. 6*A*). sICAM-1_GCN4(L43C) also showed monomeric and dimeric bands at 58 and 112 kDa, respectively (Fig. 6*A*). However, it also exhibited a third band migrating at ~180 kDa (determined below to represent ring-like dimers) and a lesser fourth band migrating at ~ 200 kDa (determined below to represent W-shaped tetramers) (Fig. 6*A*).

To characterize topology, sICAM-1_GCN4(L43C) was expressed in CHO.Lec 3.2.8.1 cells and immunoaffinity purified. In subsequent ion exchange chromatography (Fig. 6*B*, *left*), distinct forms of sICAM-1_GCN4(L43C) were enriched in different fractions as shown by nonreducing SDS-PAGE (Fig. 6*B*, *right*). Fraction 15 consisted almost entirely of the ~180-kDa form, whereas fraction 16 contained ~10, ~40, and ~50% of ~58-, ~112-, and ~180-kDa forms, respectively (Fig. 6*B*, *right*). Fraction 21 contained all four forms (~58, ~112, ~180, and ~200 kDa) in significant amounts (Fig. 6*B*). Each of these fractions (fractions 15, 16, and 21) was then subjected to glycerol gradient sedimentation. This separated the larger proteins from the monomer and resulted in fractions enriched in one, two, or three of the larger forms (Fig. 7, *A*, *C*, and *E*).

Electron microscopy of rotary-shadowed preparations showed that each of the three higher molecular mass bands seen in SDS-PAGE corresponded to a distinct topologic form of ICAM-1 (Fig. 7). Strikingly, the molecules in fraction 15, which contained only the ~180-kDa form (Fig. 7*A*), were all ring-like,

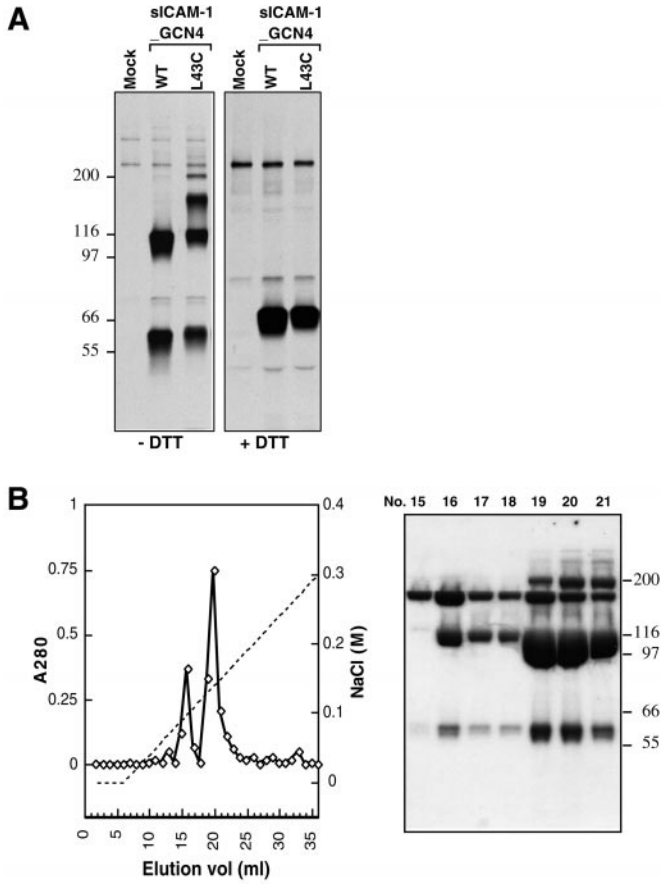

FIG. 6. **Covalently stabilized domain 1/C-terminal dimers.** The domain 1 cysteine mutation L43C was introduced into the sICAM-1_GCN4 C-terminal dimer, and the resulting domain 1/C-terminal constructs were expressed in CHO.Lec 3.2.8.1 cells. *Panel A*, ^{35}S-labeled secreted material was immunoprecipitated with R6.5 mAb, subjected to either nonreducing (−*DTT*) or reducing (+*DTT*) SDS-PAGE (8% gel), and visualized by fluorography. *Panel B*, affinity-purified sICAM-1_GCN4(L43C) was bound to a Mono Q column and eluted with a linear gradient (0–1 M) of NaCl (*left*). Fractions 15–21 were subjected to SDS-PAGE (8% gel) and Coomassie Blue staining, revealing major bands of 110, 180, and 200 kDa (*right*). Molecular weight standards are shown on the *right*.

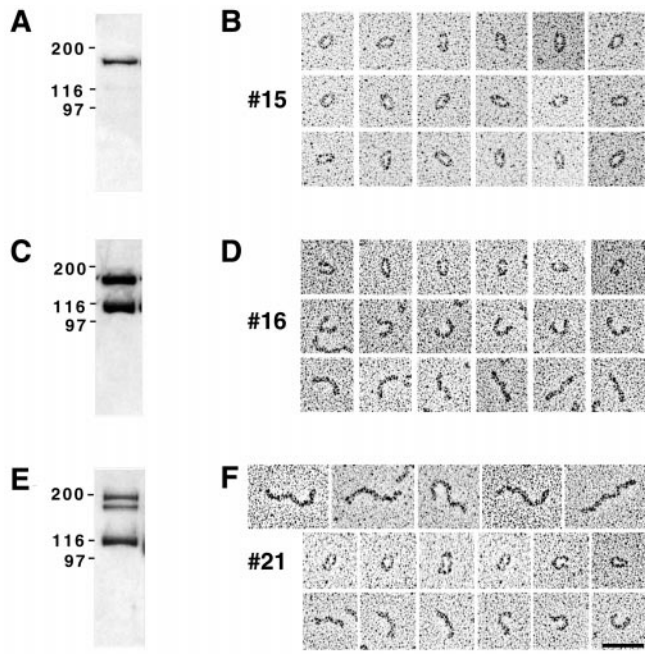

FIG. 7. **Glycerol gradient sedimentation and visualization of domain 1/C-terminal dimers.** Fractions 15, 16, and 1 from Fig. 6*B* were subjected separately to glycerol gradient sedimentation. Glycerol gradient fractions that were enriched in higher molecular weight species as shown by nonreducing SDS-PAGE (10% gel) (*panels A*, *C*, and *E*) were subjected to rotary staining and electron microscopy (*panels B*, *D*, and *F*). Representative images are shown for each fraction. *Panels A* and *B*, fraction 15; *panels C* and *D*, fraction 16; *panels E* and *F*, fraction 21. *Bar* = 50 nm. *Panel B*, fraction 15 contained ring-like, oval-shaped dimers (*all three rows*). *Panel D*, fraction 16 contained ring-like dimers (*top row*), U-shaped dimers (*middle row*), and extended dimers (*bottom row*). *Panel F*, fraction 21 contained W-shaped and extended tetramers (*top row*), ring-like dimers (*middle row*), and extended and U-shaped dimers (*bottom row*).

oval-shaped structures with a contour length (*i.e.* circumference) of 32–44 nm. This topomer is a dimer based on its length. Its ring-like shape is consistent with a "closed" conformation in which both domain 1 and C-terminal dimerization have been covalently stabilized. This topomer migrated anomalously in SDS-PAGE because the C-terminal and domain 1 dimers migrated at 112 kDa. SDS-denatured proteins normally assume long, rod-like shapes. In contrast, the ~180-kDa form would be constrained by disulfide bonds near its N and C termini to be approximately circular, which might alter the way it is sieved or oriented during electrophoresis through a polyacrylamide gel and give rise to anomalous migration in SDS-PAGE.

Glycerol gradient-purified fraction 16 contained both the ~180- and ~112-kDa bands (Fig. 7*C*) and showed two distinct topomers in electron micrographs (Fig. 7*D*). Some molecules were closed rings, identical to those found in fraction 15 (Fig. 7*D*, *top row*), and others were extended linear molecules (Fig. 7*D*, *center* and *bottom rows*). The extended dimers had lengths of ~36–40 nm and sometimes formed U shapes (Fig. 7*D*, *center row*). The closed rings were identical to those seen in fraction 15 and thus correspond to the 180-kDa form in SDS-PAGE. The linear molecules were seen in fraction 16 and not in fraction 15 and thus were identified as the ~112-kDa band. These molecules are the same mass and length as both the C-terminal dimers and the domain 1 dimers, and the linear molecules in 16 appear to be a mixture of these two forms.

Finally, three molecular species were observed in fraction 21 of ~200, ~180, and ~112 kDa in SDS-PAGE (Fig. 7*E*). Ring-like dimers ~32–38 nm in length as well as U-shaped dimers ~36–40 nm in length were observed in micrographs (Fig. 7*F*, *center* and *bottom rows*, respectively). These appear to correspond to the topomers described above which migrate at ~180 and ~112 kDa in SDS-PAGE, respectively. In addition, fraction 21 contained significant amounts of long extended molecules with irregular bends, sometimes forming W-shaped structures (Fig. 7*F*, *top row*). These correspond to the additional ~200-kDa form seen in this fraction and not in fraction 15 or 16. Based on the length of ~73–77 nm and the molecular mass of ~200 kDa, these W-shaped structures represent tetramers, in which domain 1 and C-terminal dimerization occur in *trans*, *i.e.* between different pairs of molecules.

Ligand Binding of Domain 1, C-terminal, and Domain 1/C-terminal ICAM-1 Dimers—To determine whether the domain 1 dimers, C-terminal dimers, and the ring-like, closed domain 1/C-terminal dimers retained the ability to bind ligand, we used a BIAcore to measure binding to the αL I domain. We used a recently described mutant α_L I domain with two cysteine substitutions that form a disulfide bond that locks the I domain into the open, high affinity conformation (7–9). The high affinity mutant $\alpha_L\beta_2$ I domain was immobilized on the surface of a BIAcore sensor chip. Initial experiments demonstrated specificity, in that sICAM-1 bound in a Mg^{2+}-dependent manner to chips with immobilized $\alpha_L\beta_2$ I domain and did not bind to chips with immobilized bovine serum albumin (data not shown). The domain 1 dimer, C-terminal dimer, and ring-like domain 1/C-

TABLE II

BIAcore measurements of the kinetics of dimeric and monomeric ICAM-1 binding to $\alpha_L\beta_2$ I domain

The purified mutant open, high affinity $\alpha_L\beta_2$ I domain was immobilized on a BIAcore sensor chip surface, and the binding of ICAM-1 preparations was measured under a constant flow of 10–60 μl/min in Tris-buffered saline containing 1 mM $MgCl_2$. The K_D values are expressed in mol of dimer or monomer; for expression in terms of binding sites, the K_D values of the dimers should be multiplied by 2. Curve fitting of the association and dissociation phases with BIAevaluation 3.1 software was used to calculate k_{on}, k_{off}, and K_D values. All values are expressed as the mean ± S.E. for three separate experiments, with the exception of the domain 1/C-terminal dimer for which only enough material for two experiments was generated.

ICAM-1 topology	k_{on}	k_{off}	K_D
	$M^{-1}\ s^{-1} \times 10^{-4}$	$s^{-1} \times 10^{3}$	nM
C-terminal dimer	4.11 ± 0.05	2.40 ± 0.06	58.4 ± 1.6
Domain 1/C-terminal dimer	2.94 ± 0.31	3.16 ± 0.12	109.1 ± 15.6
Domain 1 dimer	2.80 ± 0.09	1.60 ± 0.04	56.1 ± 2.1
sICAM-1 (monomer)	13.30 ± 0.60	22.60 ± 1.60	168.7 ± 5.5

terminal dimer from fraction 15 all retained specific ligand binding for the α_L I domain (Table II). Moreover, the association rate constants (k_{on}) (ranging from 28,000 to 41, 100 $M^{-1}\ s^{-1}$) and dissociation rate constants (k_{off}) (ranging from 1.6×10^{-3} to $3.16 \times 10^{-3}\ s^{-1}$) for all dimeric ICAM-1 proteins (domain 1, C-terminal, and domain 1/C-terminal dimers) were quite similar (Table II). Accordingly, the equilibrium constants (K_D) ranged from 56 to 109 nM for the ICAM-1 dimers, ~1.5–3-fold lower than that of sICAM-1 (169 nM) (Table II). Thus, there was no impairment whatsoever compared with the monomer in binding of any of the dimeric topomers to the α_L I domain. The slower k_{on} and k_{off} of the dimers compared with the monomers is a reflection of their larger size; such effects have been well documented (34, 35).

As a second measure of domain 1, C-terminal, and domain 1/C-terminal dimer function we used them to inhibit homotypic aggregation by SKW3 cells (data not shown). SKW3 cells were induced to form $\alpha_L\beta_2$- and ICAM-3-dependent homotypic cell aggregates (15) by activation of $\alpha_L\beta_2$ with the mAb CBR-LFA1/2. Aggregation performed in the presence of increasing amounts of sICAM-1 revealed effective inhibition of aggregation with an IC_{50} of ~1600 nM. Experiments with ICAM-1 dimers revealed that domain 1, C-terminal, and domain 1/C-terminal (ring-like conformers; fraction 15) dimers all inhibited aggregation with similar IC_{50} values of ~800 nM. Thus, in these assays, as with the BIAcore studies, the ICAM-1 dimers bound to $\alpha_L\beta_2$ as effectively as monomeric ICAM-1.

DISCUSSION

To function effectively, ICAM-1 must be displayed with an appropriate orientation, valence, and distribution on the cell surface so it can interact with $\alpha_L\beta_2$ on the surface of an opposing cell. Furthermore, because $\alpha_L\beta_2$ and ICAM-1 are often coexpressed on leukocytes, there must be mechanisms that favor interactions between molecules on opposite cells over interactions between molecules on the same cell. Cross-linking of ICAM-1 on the cell surface has shown a predominance of dimers over monomers and also the existence of a substantial proportion of higher order oligomers of > 200 kDa (10, 11). The mAb CA-7 specific for domain 5 of ICAM-1 was found to bind poorly to native cell surface ICAM-1 or ICAM-1 with all but two residues of the cytoplasmic domain deleted, but it bound well to ICAM-1 with a glycosylphosphatidylinositol anchor substituted for its native transmembrane domain. Furthermore, CA-7 bound well to soluble monomeric ICAM-1 but not dimeric ICAM-1 (11). These findings suggested that ICAM-1 dimerized through its transmembrane domain, in agreement with the presence of a glycine patch in helical wheel displays which favors dimerization to avoid exposure of polar carbonyl and amide backbone groups in the membrane (Fig. 1) (10, 11). The shielding of an epitope in domain 5 is consistent with its proximity to a dimerization interface in the transmembrane domain or with an additional role for domain 5 in dimerization. In a crystal structure of domains 1 and 2 of ICAM-1, a dimerization interface was revealed in domain 1 (4) which presented another possible way in which ICAM-1 could dimerize. Residues important in binding ICAM-1 to $\alpha_L\beta_2$ are on the side of domain 1 opposite to this dimerization interface; whether dimerization in domain 1 would interfere with binding to ICAM-1 was one of the issues investigated in this study. Monomeric sICAM-1 is a bent rod (2, 3); therefore, one way in which dimerization at both the C terminus and in domain 1 could be accommodated would be by formation of a ring-like dimer (4, 36).

In this study, we have for the first time investigated the architecture of ICAM-1 dimers in the electron microscope and have obtained evidence for several different ICAM-1 topologies (Fig. 8) and their functional activity. In our initial experiments, we examined ICAM-1 dimers that were linked covalently through a disulfide-bonded C-terminal α-helical coiled coil. We found that C-terminal dimers had the potential for domain 1-mediated dimerization leading to ring-like dimeric and W-shaped tetrameric topologies. U-shaped molecules were also observed, which may represent circles in which noncovalent dimerization through domain 1 was disrupted by contact with the mica (32, 33).

Previous studies suggested that in solution, dimerization through domain 1 alone was too unstable to form significant amounts of observable dimers (11). We tested whether introduction of cysteine residues into appropriate positions in the domain 1 dimer interface visualized in the crystal study would lead to the formation of disulfide-linked dimers. Indeed, cysteine mutations at several sites in domain 1 allowed formation and isolation of disulfide-linked ICAM-1 dimers. Furthermore, disulfide bonds could be formed by substitution to cysteine of Leu-42 or Leu-43, but not Leu-18 or Leu-44. In the crystal-defined dimer interface, the Cβ-Cβ distances for the former but not the latter residues were within the range optimal for disulfide bond formation of 3.41–4.25 Å (24). The latter residues were solvent-exposed and could have formed disulfides with a small shift in the monomer-monomer interface. Therefore, the specific disulfide bond formation by Leu-42 and Leu-43 suggests that disulfide bond formation was a consequence of favorable noncovalent interactions at the crystal-defined interface. These data provide evidence for domain 1-mediated dimerization of ICAM-1 in solution in a manner that is consistent with that observed previously in crystal studies (4).

We tested whether dimerization in the domain 1 interface would result in an architecture that would be compatible with simultaneous dimerization C-terminal to domain 5. Indeed, domain 1/C-terminal dimers could readily form the predicted ring-like topology. On the cell surface, an equilibrium may exist between closed ring-like and open C-terminal dimers (Fig. 8, *A* and *B*).

In addition to the ring-like domain 1/C-terminal dimers, we also observed significant amounts of W-shaped tetrameric mol-

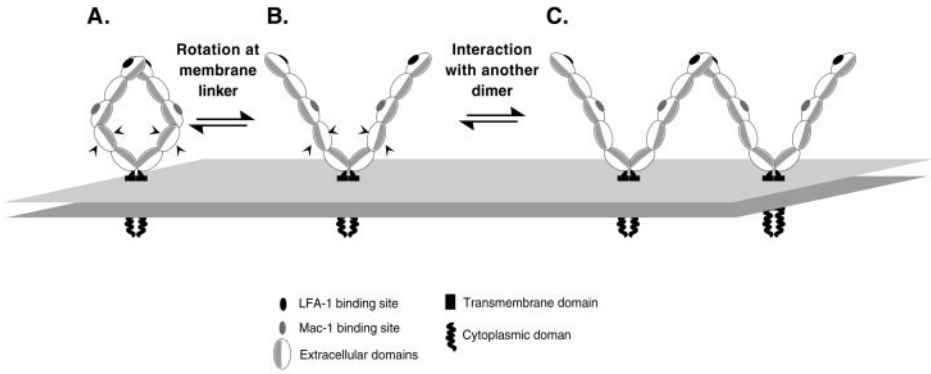

FIG. 8. **Model of ICAM-1 topomers on the cell surface.** ICAM-1 is drawn as five linked *ovals* representing domains 1–5 expressed on the cell surface (two *planes* representing the membrane bilayer). The $\alpha_L\beta_2$ binding site has been localized previously to the face of domain 1 opposite the dimerization interface (4), whereas the $\alpha_M\beta_2$ binding site is located in domain 3 (37) and is predicted to lie on the same side of the ICAM-1 molecule as the $\alpha_L\beta_2$ binding site (see Footnote 3). To maintain the same dimerization interfaces in domains 1 and 5 upon conversion from the ring-like open dimer (*A*) to the W-shaped tetramer (*C*), a rotation of ~180° and some hinge-like motions must occur in one or more of the interdomain linkages located between domains 1 and 5. In the figure, this is symbolized by rotation at the domain 4-domain 5 linkage (*circular arrows*) and a hinge-like motion at both ends of domain 4.

ecules in which domain 1 and C-terminal dimerization occurs between different pairs of molecules (Fig. 8*C*). Maintenance of the same domain 1-domain 1 and domain 5-domain 5 dimer interfaces in the ring-like dimer and in the W-shaped tetramer requires rotation at the domain 1-domain 2, domain 2-domain 3, domain 3-domain 4, or domain 4-domain 5 boundaries totaling ~180° (for simplicity shown as a rotation about the domain 4-domain 5 boundary, with hinge-like motion at both ends of domain 4 in Fig. 8). A bend has previously been visualized between domains 3 and 4 in ICAM-1 (2, 3), and most of the rotation may occur at this junction. Rotational or hinge-like movements between domains are consistent with the variation in shapes of the dimeric and tetrameric molecules visualized in this study. Interdomain movement has been visualized at the interface between domains 1 and 2 of ICAM-1 (4), and similar movements may occur at other domain interfaces.

It has been observed previously that the domain 1 dimer interface is on the opposite side of domain 1 from the $\alpha_L\beta_2$ binding face (4). Thus, it is predicted that in both the ring-like and the W-shaped structures, the $\alpha_L\beta_2$ binding surface in domain 1 would be oriented away from the cell surface, available for integrin engagement (Fig. 8). However, the compatibility of dimerization in domain 1 with ligand binding had not been tested previously. We have measured the affinity of different ICAM-1 topomers for the $\alpha_L\beta_2$ I domain. Our results show that dimerization in domain 1, C-terminal to domain 5, or at both sites did not impair binding to ICAM-1. Indeed, when corrected for the presence of 2-fold more binding sites, the affinities of the dimers for the I domain are within 1.5-fold of monomeric sICAM-1.

The topologies we have defined have important implications for the function of ICAM-1 in cell adhesion. Interactions through domain 1 in the ring-like dimer and W-shaped tetramer will provide constraints on orientation on the cell surface (Fig. 8). Additional constraints may be provided by the putative dimerization interface in domain 5 which masks the CA-7 epitope. Because of symmetry considerations, it is reasonable to conclude that the 2-fold rotational symmetry axis within the domain 1 dimer interface will be oriented perpendicular to the membrane, as shown in Fig. 8. This will present the binding site in domain 1 optimally for binding to $\alpha_L\beta_2$ on an opposing cell, either in the ring-like dimer or in the tetramer configuration (Fig. 8). We predict that the binding site for $\alpha_M\beta_2$ in domain 3 of ICAM-1 (37) is on the same face of ICAM-1 and would also be well exposed in both dimers.[3] However, the height above the membrane and orientation of these binding interfaces could differ among the ring-like dimer, open dimer, and W-tetramer, and thus interconversion among these topomers could have important consequences for regulating cell adhesion. For example, binding of $\alpha_L\beta_2$ to domain 1 and $\alpha_M\beta_2$ to domain 3 might be affected differently. Moreover, the W tetramers are available for further multimerization through domain 1, and thus long strings of ICAM-1 molecules could be built up which could have important implications for avidity regulation of cell adhesion.

REFERENCES

1. Dustin, M. L., and Springer, T. A. (1999) in *Guidebook to the Extracellular Matrix and Adhesion Proteins* (Kreis, T., and Vale, R., eds) 2nd Ed., pp. 228–232, Sambrook and Tooze, New York
2. Staunton, D. E., Dustin, M. L., Erickson, H. P., and Springer, T. A. (1990) *Cell* **61,** 243–254
3. Kirchhausen, T., Staunton, D. E., and Springer, T. A. (1993) *J. Leukocyte Biol.* **53,** 342–346
4. Casasnovas, J. M., Stehle, T., Liu, J.-h., Wang, J.-h., and Springer, T. A. (1998) *Proc. Natl. Acad. Sci. U. S. A.* **95,** 4134–4139
5. Bella, J., Kolatkar, P. R., Marlor, C., Greve, J. M., and Rossmann, M. G. (1998) *Proc. Natl. Acad. Sci. U. S. A.* **95,** 4140–4145
6. Stewart, M., and Hogg, N. (1996) *J. Cell. Biochem.* **61,** 554–561
7. Lu, C., Shimaoka, M., Ferzly, M., Oxvig, C., Takagi, J., and Springer, T. A. (2001) *Proc. Natl. Acad. Sci. U. S. A.* **98,** 2387–2392
8. Shimaoka, M., Lu, C., Palframan, R., von Andrian, U. H., Takagi, J., and Springer, T. A. (2001) *Proc. Natl. Acad. Sci. U. S. A.* **98,** 6009–6014
9. Lu, C., Shimaoka, M., Zang, Q., Takagi, J., and Springer, T. A. (2001) *Proc. Natl. Acad. Sci. U. S. A.* **98,** 2393–2398
10. Reilly, P. L., Woska, J. R., Jr., Jeanfavre, D. D., McNally, E., Rothlein, R., and Bormann, B.-J. (1995) *J. Immunol.* **155,** 529–532
11. Miller, J., Knorr, R., Ferrone, M., Houdei, R., Carron, C. P., and Dustin, M. L. (1995) *J. Exp. Med.* **182,** 1231–1241
12. Labadia, M. E., Jeanfavre, D. D., Caviness, G. O., and Morelock, M. M. (1998) *J. Immunol.* **161,** 836–842
13. Casasnovas, J. M., and Springer, T. A. (1995) *J. Biol. Chem.* **270,** 13216–13224
14. Janin, J. (1997) *Nat. Struct. Biol.* **4,** 973–974
15. de Fougerolles, A. R., Qin, X., and Springer, T. A. (1994) *J. Exp. Med.* **179,** 619–629
16. Rothlein, R., Czajkowski, M., O'Neil, M. M., Marlin, S. D., Mainolfi, E., and Merluzzi, V. J. (1988) *J. Immunol.* **141,** 1665–1669
17. Rothlein, R., Mainolfi, E. A., Czajkowski, M., and Marlin, S. D. (1991) *J. Immunol.* **147,** 3788–3793
18. Maio, M., Tessitori, G., Pinto, A., Temponi, M., Colombatti, A., and Ferrone, S. (1989) *J. Immunol.* **143,** 181–188
19. Parkos, C. A., Colgan, S. P., Diamond, M. S., Nusrat, A., Liang, T. W., Springer, T. A., and Madara, J. L. (1996) *Mol. Med.* **2,** 489–505
20. Staunton, D. E., Merluzzi, V. J., Rothlein, R., Barton, R., Marlin, S. D., and Springer, T. A. (1989) *Cell* **56,** 849–853
21. Seed, B. (1987) *Nature* **329,** 840–842
22. Harbury, P. B., Zhang, T., Kim, P. S., and Alber, T. (1993) *Science* **262,** 1401–1407
23. Wagschal, K., Tripet, B., and Hodges, R. S. (1999) *J. Mol. Biol.* **285,** 785–803

[3] T. A. Springer, C. Jun, and J. Wang, unpublished data.

24. Hazes, B., and Dijkstra, B. W. (1988) *Protein Eng.* **2,** 119–125
25. Levitt, M. (1992) *J. Mol. Biol.* **226,** 507–533
26. Marlin, S. D., Staunton, D. E., Springer, T. A., Stratowa, C., Sommergruber, W., and Merluzzi, V. (1990) *Nature* **344,** 70–72
27. Takagi, J., Erickson, H. P., and Springer, T. A. (2001) *Nat. Struct. Biol.* **8,** 412–416
28. Oxvig, C., Lu, C., and Springer, T. A. (1999) *Proc. Natl. Acad. Sci. U. S. A.* **96,** 2215–2220
29. Casasnovas, J. M., and Springer, T. A. (1994) *J. Virol.* **68,** 5882–5889
30. Fowler, W. E., and Erickson, H. P. (1979) *J. Mol. Biol.* **134,** 241–249
31. Rothlein, R., and Springer, T. A. (1986) *J. Exp. Med.* **163,** 1132–1149
32. Carrell, N. A., Erickson, H. P., and McDonagh, J. (1989) *J. Biol. Chem.* **264,** 551–556
33. Schürmann, G., Haspel, J., Grumet, M., and Erickson, H. P. (2001) *Mol. Biol. Cell* **12,** 1765–1773
34. de Mol, N. J., Plomp, E., Fischer, M. J., and Ruijtenbeek, R. (2000) *Anal. Biochem.* **279,** 61–70
35. Schuck, P. (1996) *Biophys. J.* **70,** 1230–1249
36. Wang, J.-h., and Springer, T. A. (1998) *Immunol. Rev.* **163,** 197–215
37. Diamond, M. S., Staunton, D. E., Marlin, S. D., and Springer, T. A. (1991) *Cell* **65,** 961–971
38. Kabsch, W., and Sander, C. (1983) *Biopolymers* **22,** 2577–2637